OFFICE OF NAVAL RESEARCH

GRANT or CONTRACT: N00014-91-J-1919

96PRO-2855
Robert Nowak

Technical Report No. 24

Atomic Level Studies of Se Electrodeposition on Au(111) and Au(110)

Tedd E. Lister and John L. Stickney

In press in

the

Journal of Physical Chemistry

Department of Chemistry
University of Georgia
Athens, GA 30602-2556

10/15/96

DISCLAIMER NOTICE

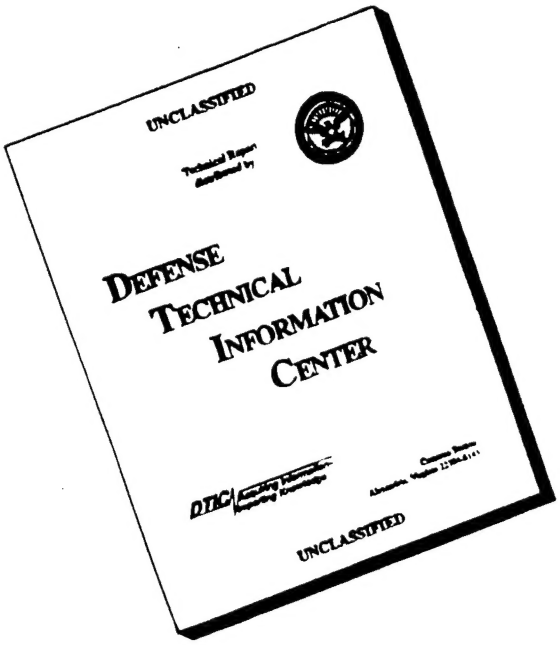

THIS DOCUMENT IS BEST QUALITY AVAILABLE. THE COPY FURNISHED TO DTIC CONTAINED A SIGNIFICANT NUMBER OF PAGES WHICH DO NOT REPRODUCE LEGIBLY.

REPORT DOCUMENTATION PAGE

Form Approved
OMB No. 0704-0188

1. AGENCY USE ONLY (Leave blank)	2. REPORT DATE	3. REPORT TYPE AND DATES COVERED
	10/15/96	Technical 6/1/95 - 10/15/96

4. TITLE AND SUBTITLE
Atomic Level Studies of Se Electrodeposition on Au(111) and Au(110)

5. FUNDING NUMBERS
G-N00014-19-J-1919
Dr. Robert J. Nowak
96PRO-2855

6. AUTHOR(S)
Tedd E. Lister and John L. Stickney

7. PERFORMING ORGANIZATION NAME(S) AND ADDRESS(ES)
John L. Stickney
Department of Chemistry
University of Georgia
Athens, GA 30602-2556

8. PERFORMING ORGANIZATION REPORT NUMBER
Technical Report #24

9. SPONSORING/MONITORING AGENCY NAME(S) AND ADDRESS(ES)
Office of Naval Research
Chemistry Division
800 North Quincy Street
Arlington, VA 22217-5660

10. SPONSORING/MONITORING AGENCY REPORT NUMBER

11. SUPPLEMENTARY NOTES

12a. DISTRIBUTION/AVAILABILITY STATEMENT
Approved for public release and sale; its distribution is unlimited

12b. DISTRIBUTION CODE

13. ABSTRACT *(Maximum 200 words)*

Studies of the electrodeposition of Se atomic layers of Au(111) and Au(110) are presented. Three electrochemical methods of forming Se atomic layers were investigated: reductive deposition, oxidative stripping of bulk Se, and reductive stripping of bulk Se. The resulting Se atomic layers were studied using low energy electron diffraction (LEED), Auger electron spectroscopy (AES), and scanning tunneling microscopy (STM). LEED indicated the formation of Au(111) ($\sqrt{3}$X$\sqrt{3}$)R30°-Se and Au(110)(2X3)-Se structures. STM analysis confirmed the presence of those structures along with several others. At low Se coverages on Au(111), a mosaic structure was formed, composed of a large number of small domains of a ($\sqrt{3}$X$\sqrt{3}$)R30°-Se structure, separated by areas void of Se. At higher coverages, near 1/3, the ($\sqrt{3}$X$\sqrt{3}$)R30° structure covered most of the surface, except for a number of linear phase boundaries. Commensurate with completion of the ($\sqrt{3}$X$\sqrt{3}$)R30° structure, some domains of square Se_8 rings were usually evident, as well. At still higher coverages, a heterogeneous surface was formed, composed of a complex network of rings, chains, clusters and pits. This heterogeneity appears to result from slow deposition kinetics, probably the result of both a low exchange current and Se surface mobility.

14. SUBJECT TERMS
Se, UPD, STM, LEED, Electrodeposition

15. NUMBER OF PAGES
41

16. PRICE CODE

17. SECURITY CLASSIFICATION OF REPORT	18. SECURITY CLASSIFICATION OF THIS PAGE	19. SECURITY CLASSIFICATION OF ABSTRACT	20. LIMITATION OF ABSTRACT
Unclassified	Unclassified	Unclassified	UL

Submitted to J. Phys. Chem.

ATOMIC LEVEL STUDIES OF Se ELECTRODEPOSITION ON Au(111) AND Au(110)

T.E. Lister and J.L. Stickney*

Department of Chemistry, University of Georgia, Athens, Georgia 30602

* To Whom Correspondence should be addressed

ABSTRACT

Studies of the electrodeposition of Se atomic layers on Au(111) and Au(110) are presented. Three electrochemical methods of forming Se atomic layers were investigated: reductive deposition, oxidative stripping of bulk Se, and reductive stripping of bulk Se. The resulting Se atomic layers were studied using low energy electron diffraction (LEED), Auger electron spectroscopy (AES), and scanning tunneling microscopy (STM). LEED indicated the formation of Au(111)(✓3X✓3)R30°-Se and Au(110)(2X3)-Se structures. STM analysis confirmed the presence of those structures along with several others. At low Se coverages on Au(111), a mosaic structure was formed, composed of a large number of small domains of a (✓3X✓3)R30°-Se structure, separated by areas void of Se. At higher coverages, near 1/3, the (✓3X✓3)R30° structure covered most of the surface, except for a number of linear phase boundaries. Commensurate with completion of the (✓3X✓3)R30° structure, some domains of square Se_8 rings were usually evident, as well. At still higher coverages, a heterogeneous surface was formed, composed of a complex network of rings, chains, clusters and pits. This heterogeneity appears to result from slow deposition kinetics, probably the result of both a low exchange current and Se surface mobility. Some of the kinetic sluggishness may have resulted from the need to convert whole domains of Se atoms from one site to another, in order to remove phase boundaries. STM studies of the Au(110) surface indicated that only the (2X3) structure was formed at coverages much below 1 monolayer, and that it was formed homogeneously. At coverages above a monolayer, a honeycomb structure composed of chains of Se atoms was observed, which filled in at still higher coverages to complete a second Se layer.

INTRODUCTION

The chalcogenides are an important and interesting class of adsorbates. The oxides are, of course, well studied for obvious reasons. The surface chemistry of sulfur on metals has also been studied, as S is a well known catalyst poison. The adsorption of S and Se on III-V compound semiconductor surfaces is gaining importance, as they acts as capping layers [1,2]. Furthermore, studies of self assembled monolayers (SAMs) on Au have increased dramatically in the last few year, and so has the importance of understanding the binding of S to Au. Studies of Te and Se adsorption at metal surfaces are increasing as well [3-11].

Generally, metal monolayers deposited on metal surfaces form close packed adlattice, as long as no other adsorbates are involved. On the other hand, the surface chemistry of the main group elements show significantly more variety. The halides, for instance, frequently adopt multiple structures on a given plane, as a function of coverage [12-17]. The structures of halide atomic layers tend to be hexagonal, or quasi hexagonal, compression structures with an apparent low degree of inter-halide bonding. However, some chain formation has been observed for high coverages of I, apparently the beginning of a bulk poly-iodide phase [15].

The chalcogenides show an even more diverse assortment of surface structures than the halides, including: close packed layers [5,6], dimers [3-6], trimers [18], chains [3,4], and rings [19,20]. Some of those studies involved chalcogenides adsorbed from the gas phase in UHV, however, the range of coverages and structures achievable in UHV appears more limited then corresponding electrochemical studies [21]. Electrodeposition provides a high degree of control over chalcogenide coverage, and thus access to a larger array of different surface structures. Studies of the these structures are facilitated by the ability to perform STM studies in air of chalcogenide layers on some metal surfaces. The chalcogenides are fairly stable in air, so

structures formed in solution on noble metals can usually be emersed (removed from solution) and imaged in air. In addition, chalcogenide layers can be imaged while they are forming, *in situ* (in solution, under potential control).

As mentioned above, chalcogenide adsorption is of interest for a number of reasons. Work in our group involves the electrochemical formation of II-VI compound semiconductors. Chalcogenide atomic layers are important as the electrochemical analog of atomic layer epitaxy (ALE) is being used to form the compounds [22,23]. ALE is a methodology used to form thin films of materials an atomic layer at a time, based on the use of surface limited reactions. The electrochemical analog is also based on surface limited reactions, referred to as underpotential deposition (UPD) [24]. This paper describes studies of the formation of the first atomic layer of Se, the "UPD" layer, on two of the low index plans of Au: the (111) and the (110). Similar studies performed on Au(100) are described elsewhere [5,6]. Studies of Te UPD have been published as well [3,4], as have papers describing structures formed by S on Au [25,26].

The present studies are intended to provide an understanding of the structures and compositions of Se atomic layers formed under various electrochemical conditions. This information should then help in development of electrochemical ALE (ECALE) [27-32] growth cycles for II-VI compounds such as CdSe [33,34] and ZnSe.

EXPERIMENTAL

An ultra-high vacuum-electrochemical instrument (UHV-EC) was used to perform some of the experiments described below [35]. The instrument consisted of a UHV surface analysis chamber coupled directly to an antechamber containing an electrochemical cell. The main chamber contained surface analytical probes, such as: Auger electron spectroscopy (AES) (Physical Electronics), and low energy electron diffraction (LEED) (Physical Electronics). Prior to each UHV-EC experiment, the substrate was cleaned by ion bombardment, annealed to a faint orange glow and analyzed using LEED and AES. The substrate was then transferred to the electrochemical antechamber and back-filled with Ar gas (99.99%). Following electrodeposition, the antechamber was pumped down and the substrate was transferred back to the main chamber.

A Digital Instruments Nanoscope III was used for the STM experiments. Deposits studied by STM were formed in a simple electrochemical H-cell. STM imaging was performed both in air and *in situ*. STM tips were formed from tungsten wire, etched in 1 M KOH solution at 12 VAC. Tips used for *in situ* experiments were first coated with hot polyethylene, in a manner similar to that used to coat tips with Apiezon wax [36].

The Au substrates were single crystals, oriented to their respective low index planes using Laue back reflection X-ray diffraction. After mechanically polishing to the desired planes, they were briefly electropolished at constant current using a cyanide bath [37]. Three substrates were used in this study. In the UHV-EC experiments, a "Tri" crystal was used. The Tri crystal consisted of a Au single crystal oriented and polished on three sides, each to a different low index plane. In addition to the Tri crystal, (111) and (110) round Au single crystal slices, polished on

both sides, were used for STM studies. The crystals used for STM studies were pre-treated before each deposition using a methane/oxygen flame to clean and anneal the surface.

All chemicals used were reagent grade or better. Water was from a Nanopure system, fed by the house distilled water line. The Se deposition solution was composed of 1 mM SeO_2 (Johnson Matthey) and 20 mM H_2SO_4 (Baker Analyzed) (pH 2.2). Solutions used for reductive stripping of bulk Se were composed of 5 mM sodium borate (Allied Chemical) (pH 9.0). All solutions were purged with Ar or N_2 gas (99.99%). All potentials are referenced to a Ag/AgCl (1 M KCl) reference electrode.

RESULTS AND DISCUSSION

Se Voltammetry and Formation of Se Atomic Layers

A voltammogram of the Au tri crystal in the Se deposition solution is shown in Figure 1. Scanning from 0.60 V, $HSeO_3^-$ reduction begins near 0.40 V in a surface limited feature that resembles a UPD peak (C_1). The subsequent deposition feature (peak C_2) also appears to be surface limited. C_2 is less like a UPD feature then C_1, as more then two monolayers of Se have been deposited by its conclusion. Although not shown, scanning below 0 V results in further Se deposition. The presence of irreversibility in the voltammetry is evident when the potential scan is reversed at 0 V. Se oxidative stripping occurs in two peaks, a bulk stripping feature at 0.55 V (peak A_2), and a UPD stripping feature at 0.70 V (peak A_1).

The irreversibility evident between deposition and stripping features in Figure 1, over 0.3 V, indicates that peak C_1 does not occur at an underpotential at all. An open circuit potential of 0.41 V was measured for a Au(111) crystal on which bulk Se had been deposited at -0.2 V,

indicating the formal potential for Se is near 0.41 V. Evidently, both of the surface limited deposition peaks in Figure 1 occur at overpotentials. It has been suggested that the high resistivity of Se (10^{10} ohm-cm) may be limiting the deposition [5,6], however, the resistance of a single atomic layer of Se should be far from that necessary to produce the observed potential shift.

Three methods of electrodepositing Se atomic layers have been identified [5,6]. A first is straight forward, involving scanning the electrode potential into peak C_1 and holding the potential until an atomic layer of Se had been deposited. A second involves oxidation of bulk Se (formed in a previous step of depositing peaks C_1 and C_2). The potential was adjusted to 0.7 V (between peaks A_1 and A_2) where bulk Se is oxidatively stripped, leaving only an atomic layer. The final method also involves stripping bulk Se to leave an atomic layer, however, after deposition the solution was exchanged for 5 mM sodium borate (no H_2SeO_3) and the potential was shifted negatively to -0.7 V, where the bulk Se was converted to selenide, leaving only an atomic layer. The solution was exchanged in order to avoid conproportionation at low potentials, that occurs if H_2SeO_3 is present in the cell when Se^{2-} is generated. The H_2SeO_3 reacts with the Se^{2-} to form Se nuclei:

(1) $2H_2Se + H_2SeO_3 <===> 3\ Se^{\circ} + 3\ H_2O$.

Detailed coulometric studies of all three electrodeposition methods have been previously reported, concerning a Au(100) crystal [5,6].

UHV-EC studies of Se Atomic Layers

Se atomic layers formed on the Au tri-crystal were investigated using LEED and AES in the UHV-EC system. Quantitative determination of Se coverages with AES was not attempted, as

the Auger yield for Se is very low. The Auger signal for Se was clearly detected at 95 eV, but was small and overlapped with a weak Au transition (99 eV), making quantification difficult. To estimate the coverage in each experiment the crystal was electrochemically stripped in the Se deposition solution, after surface analysis. AES was, however, used to insure that no contaminates or emersed electrolytes were present on the surfaces.

LEED patterns were observed on both the Au(111) and Au(110) surfaces after formation of Se atomic layers, by each of the three electrodeposition methods. A single pattern was observed on each surface, in contrast to Se atomic layers formed on Au(100), where four distinct patterns were observed [5,6]. A (✓3X✓3)R30^0 LEED pattern (Figure 2A) was produced on Au(111), but with a relatively large amount of diffuse intensity under all the conditions investigated. In the reductive deposition experiments, the highest quality LEED patterns were observed for deposits formed by holding the potential near the peak of C_1. If the potential was held near the onset of C_1, a simple (1X1) pattern with some diffuse background intensity was observed. If the electrode potential was held in the valley between C_1 and C_2, the (✓3X✓3)R30^0 LEED pattern became very faint or non-existent. Only diffuse intensity was obtained after emersing at potentials corresponding to C_2. The (✓3X✓3)R30^0 pattern was also observed over limited stripping potential ranges, after both anodic or cathodic stripping of bulk Se. After anodic stripping at potentials between 0.60 and 0.70 V, a weak (✓3X✓3)R30^0 LEED pattern was observed. After cathodic stripping at potentials near -0.65 V, a similar (✓3X✓3)R30^0 LEED pattern was observed.

A (2X3) LEED pattern was observed on Au(110) (Figure 2B) after formation of Se atomic layers by each of the three methods. For reductive deposition, the highest quality patterns

were observed after deposition to the peak of C_1. Se deposited to potentials just past the onset of C_1 resulted in a diffuse (1X1) patterns, while deposition to the valley between C_1 and C_2 yielded a diffuse (2X3) pattern. Deposition into C_2 resulted in only diffuse intensity. Unlike Au(111), however, quality LEED patterns for anodic and cathodic stripping of bulk Se were obtained over relatively large potential ranges. For anodic stripping, the best patterns were obtained when the potential was held near the onset of bulk stripping, 0.55 V. For cathodic stripping, the best patterns were observed near -0.62 V, 100 mV below the onset of reductive stripping.

STM of Se Atomic Layers Formed on Au(111)

The LEED studies, described above, indicated the formation of only one structure on Au(111), a (✓3X✓3)R30°-Se, after deposition to the peak of C_1. STM studies, under similar deposition conditions, revealed a structure corresponding to the (✓3X✓3)R30° LEED pattern (Figure 3A). Atomic spacings measured in several images ranged from 0.48 to 0.52 nm, in good agreement with the ✓3 distance of Au (✓3 X 2.88 nm or 0.50 nm). A proposed structure is shown in Fig. 4A, where Se atoms are placed in high coordinate (three-fold) sites, at 1/3 coverage.

At coverages corresponding to those that resulted in the (✓3X✓3)R30° LEED pattern, larger scale STM images seldom displayed a simple homogeneous coverage of the structure shown in Figure 3A. Instead, surfaces supporting the (✓3X✓3)R30° structure generally included defect features and domains of a higher coverage structure, as well (Figure 3B). Some defects in Figure 3B appear as triangular shaped depressions in the (✓3X✓3)R30° structure. These triangles are randomly distributed across the surface in a single orientation and measure 4 - 6 nm

on a side. The depressions that compose the edges of the triangles appear to result from increased Se atomic spacings, due to the atoms of the (√3X√3)R30^0 structure shifting into different three-fold sites to form phase-boundaries (Figure 4B). Shifting from a √3 position to the next closest site would result in an inter atomic spacing shift from 0.50 nm to 0.68 nm, which is very close to distances measured from the triangle images. Another defect feature is shown in Figure 3C, and consists of two parallel depression lines in the terraces covered with the (√3X√3)R30^0 structure. The lines always align themselves down Au atomic rows, and always turn at angles close to 120^0. The lines are spaced about 1.8 nm apart, and originate at step edge defects or pits. These line defects are most common when the coverage is between 0.30-0.35 monolayers. A further observation is that the defects are not generally observed on regions of the crystal with a step width of less then 20 nm. It is probable that these lines are phase boundaries, like in the triangles, where domains of the (√3X√3)R30^0 structure, in different sites, come together. It can be envisioned, that as the coverage is increased, one domain starts to predominate, so phase boundaries shrink. Eventually, only a small domain of a (√3X√3)R30^0 structure in the wrong site is left, trapped. As the lines only intersect at 120° or 60°, a triangular domain results as the smallest domain possible (Figure 4B).

Figure 3D is an image of one of the brighter Se domains evident in Figure 3B, and indicates that they is composed of square Se rings. The rings measure 0.53 to 0.55 nm on a side, with their strongest intensity at the corners. Some images (Figure 3E) show eight distinct atoms in a ring or Se_8 molecule. The Se-Se bond length in the rings is 0.26-0.27 nm, slightly smaller than the Au-Au spacing in the substrate (0.288 nm). The image in Figure 3B shows that three orientations of the bright Se_8 domains are possible, rotated by 120°. The rows of Se_8 molecules

align with one of the substrate rows of Au atoms. Figure 3D shows how the rings line up perfectly along the Au rows, running diagonally from the upper left to the lower right of the image. However, the rows of Se_8 molecules perpendicular to the aligned direction lose their commensurate nature. Following a row of rings in this direction (Figure 3D), they appear to stagger back and forth about 1/2 a Se-Se distance for every ring, with a periodicity of about 6 rings. This staggering is probably a mechanism for placing the Se atoms of the square rings in the best coordination sites on the hexagonal Au(111) surface. Note that many rings are distorted from their nominal square shape, as corners of the Se_8 molecules shift from unstable top sites.

The Se ring structures were measured to be 0.08-0.12 nm higher than surrounding $(\surd 3X\surd 3)R30^0$-Se structure, leading to the conclusion that the ring domains are not a second layer of Se on the $(\surd 3X\surd 3)R30^0$-Se structure, but are in the same layer as the Se atoms making up the $(\surd 3X\surd 3)R30^0$-Se. The height difference may result from a higher tunneling probability from the ring atoms, relative to atoms of the $(\surd 3X\surd 3)R30^0$ structure. A proposed structure for the Se_8 rings is shown in Figure 4C. It is assumed that the Se atoms reside in the highest coordination sites when ever possible.

Se_8 is a stable allotrope of Se, however the bulk Se_8 ring structure involves a boat conformation with an average bond length of 0.23 nm and bond angles of 105.7^0 [38]. The Se_8 squares on the surface (Figure 3E) are dramatically altered from that bulk structure. One can account for the stability of the Se_8 square structures on the surface by noting the formation of a number of Se-Au bonds. The fact that Se_8 rings are partially commensurate with the Au surface is another indication of the importance of the substrate-adsorbate interaction.

Similar square Se_4 rings were formed by Se electrodeposition on Au(100) [5,6]. Square rings of sulfur have been observed on Au(111), after electrooxidation of Na_2S [19] or by exposure to solutions of Na_2S, SCN, and n-octadecanethiol [20]. As with the Se rings, the S-S bond distances of the S square rings appear greater than corresponding bond lengths found in bulk S_8 (0.207 nm) [38]. Some controversy existed over the assignment of the ring element, whether it was S_8 or a reconstruction of the Au surface [19,20]. Surface enhanced Raman spectroscopic (SERS) studies, however, indicated that the electrogenerated rings have spectral features consistent with S_8 rings [19].

The mixed Se structures described above were formed by deposition to the peak of C_1, and Se coverages of 0.3-0.4 monolayers. For Se deposits formed by holding at the positive edge of C_1 (just past the current onset), insufficient Se was deposited to form the $(\surd 3 X \surd 3)R30^0$ structure across the entire surface. In addition, atomic resolution images were difficult to obtain using the conditions of the images in Figure 3. Often the STM images contained horizontal noise, probably due to movement of Se atoms by the STM tip, since the Se atoms at these low coverages where not "locked" into a close packed structure like the $(\surd 3 X \surd 3)R30^0$. Occasionally, the hexagonal Au atom array of the Au(111) surface was observed on low coverage surfaces (Figure 5A). If, however, higher resistance tunneling conditions were used (set-point < 1 nA, bias > 100 mV) to study deposits near 1/5 of a monolayer, mosaic structures such as those shown in Figures 5B and C were observed. The mosaic appears as thin parallel thin lines, 0.80 nm wide and 0.20-0.23 nm high, relative to the terrace atoms. Three orientations exist for the lines, each rotated by 120^0. Atomic resolution of the mosaic structure is shown in Figure 5C, where the inter-atomic spacings were measured to be 0.45-.50 nm. Apparently, these images are initial

small domains of the (√3X√3)R30°-Se structure, covering only portions of the Au surface, and leaving significant fractions bare, as not enough Se is present to form the (√3X√3)R30° structure over the entire surface. The mosaic structure starts to coalesce at coverages over 1/4 of a monolayer, forming large domains of the (√3X√3)R30°. As the mosaic structure starts to coalesce, (√3X√3)R30° structure with line defects (Figure 3C) is observed. It is difficult, however, to form a homogeneous (√3X√3)R30°-Se deposit across the whole surface, since while the last phase boundaries are removed, domains of the Se_8 molecules are already appearing on the surface.

This demonstrates a basic problem with forming the (√3X√3)R30°-Se. The mosaic structure may be thought of as a distribution of nucleation sites on the Au surface. As the coverage grows, these domains meet and if they have initially formed in different 3 fold sites, a phase boundary is formed. The only way to remove the phase boundary is to shift all the atoms of the second domain to sites equivalent to those occupied by Se atoms in the first domain. This difficulty in converting all the domains to equivalent sites may be partially responsible for the slow kinetics observed.

When Se is deposited on Au(111) at potentials between C_1 and C_2, the surface morphology becomes even more complex. The initial surface composed of domains of (√3X√3)R30° and Se_8 rings (Figure 3B) evolves into a surface which still has some (√3X√3)R30° domains, but the domains of Se_8 rings begin to meet and become much less ordered (Figure 6A and B). Instead of arrays of rings, clusters of Se atoms are formed. The nature of these clusters is not clear, but the Se-Se atomic spacing is about 0.32 nm, apparently longer than that in the Se_8 rings (0.27 nm). The visible surface atom density of the clusters

structure thus appears lower then the density in the Se_8 ring structures observed at a lower overall Se coverage. Probably, not all the Se atoms in the clusters are visible, and the atomic density is higher then for the Se_8 ring structure. Measurement of the height of the clusters, however, relative to the surrounding ($\surd3X\surd3$)R30^0 domains on the same terraces, indicates that the clusters are only about 0.12 nm higher, similar to the Se_8 rings, not 0.3 nm which might be expected if Se atoms were stacking on each other. As with the Se_8 rings, all the Se atoms in the clusters are probably in contact with the Au substrate, but too tightly packed to resolve individually in the image.

At deposition potentials just into C_2, Se forms chains of atoms, approximately 0.30 nm apart, which grow in three directions on the surface (Fig. 6C). A second larger scale image of these chains is shown in Figure 6D, where over a monolayer of Se was deposited. A Se chain structure is not unanticipated, considering that the most stable form of Se is a helical chain structure (Se_x) [38]. The surface in Figure 6D has pits which are 0.15 - 0.20 nm deep, with chains present inside the pits, indicating that a second layer of Se may have formed. The pit edges are not rounded off, but are composed of straight Se chains intersecting at 120^0 angles. Deposits with coverages higher than shown in Figure 6D were not imaged in the present study.

Some *insitu* experiments were performed as well. That is, experiments where Se layers were imaged in solution, under potential control. The cathodic stripping of Se was imaged in one *in situ* experiment. A Au(111) electrode coated with 0.45 monolayers of Se was mounted in the *in situ* STM cell [39], in a 20 mM H_2SO_4 solution. The potential was scanned negatively, resulting in the images shown in Figures 7A-E. Figure 7A was obtained at -0.2 V, where Se is

expected to be stable. At -0.4 V (Figure 7B) some pit formation is evident, as the first changes in the surface. In Figure 7C, much clearer atomically resolved images were obtained at -0.5 V, and the pits increased in size. A portion of Figure 7C (Figure 7D) displays two structures: the (√3X√3)R30^0 and one comprised of loosely packed Se trimers. The Se-Se spacing in the trimers is essentially that of the (√3X√3)R30^0, about 0.5 nm. But the trimer structure has a (2√3X2√3)R30°-Se unit cell, at 1/4 coverage, as if one out of every four of the atoms in a (√3X√3)R30^0-Se structure had been removed. Similar S trimers have also been observed on Re(0001), after dosing with S in vacuum, all though at a slightly higher coverage [18].

Scanning to -0.70 V (Figure 7E) resulted in loss of atomic resolution, but the pits formed at -0.5 V were still evident. Further scanning of the potential to -1.2 V resulted in no significant changes in the images. Pit formation appears to result from the cathodic stripping of Se from the surface, possibly resulting from the dissolution of a small amount of the Au, as well. The amount of dissolving Au is probably a function of the amount of excess Se and the stoichiometry of any Au-Se complex involved in the dissolution step. Similar conclusions have been drawn by other workers studying Au(111) surfaces exposed to a Na_2S solution, where Au removal was detected using a quartz crystal micro-balance (QCM) [20].

STM Studies of Se Atomic Layers on Au(110)

Well ordered Se adlattices were observed with STM to form on Au(110), however the structures showed significantly less diversity than on the other two Au low index planes. The STM image shown in Figure 8A, for instance, was obtained by cathodic deposition of Se to the

peak of C_1. The unit cell is a (2X3), agreeing with the observed LEED pattern (Figure 2B). Atoms of the (2X3) are running diagonal from the lower left to the upper right side of the image, in the [110] direction. As with many structures that form on the (110) faces of cubic metals, the adsorbate atoms sit in the troughs of the surface, which run in the [110] direction, where they can achieve the highest coordination to the substrate atoms. A proposed model for the Au(110)(2X3)-Se structure is shown in Figure 9. The image in Figure 8A also shows a vertical modulation of 0.02 - 0.03 nm between adjacent Se atoms in every other row. As suggested in Figure 9, the higher atoms are probably sitting in two fold sites and the lower atoms in four fold sites in the trough. Less corrugation, however, is observed in the other, alternate, rows, where all the atoms appear to reside at approximately the same height, in nearly identical sites. The interatomic Se spacings down these alternate rows, however, are unequal, with interatomic distances alternating between about 0.41 and 0.46 nm. From the structure shown in Figure 9, it is evident why the two distances occur, as none of the atoms in these alternate rows have stable high coordinate sites, so pairs of Se atoms tend to either roll together or apart, resulting in the alternated Se-Se spacings. Images of this (2X3) structure have been obtained from deposits formed by each of the three deposition methods. Figure 8B is an STM image of the (2X3) formed by anodic stripping at 0.55 V. In that image the [110] direction runs vertically.

At coverages above one monolayer, a honeycomb structure is observed (Figure 8C). In that image, the [110] direction runs diagonally from the bottom left to upper right. The image can also be thought to consist of Se atom chains that run in the [100] direction (90° from the [110]). In some images, at slightly higher Se coverages, the honeycomb structure starts to go away. The holes in the honeycomb appear to fill in with Se atoms. Given that the Se coverage is greater then

a monolayer, it is probable that there are two layers of Se atoms at that point, the first being the (2X3) structure (Figure 9). The honeycomb is then the first step in forming the second layer of Se atoms, and filling in the holes in the honeycomb completes it.

CONCLUSION

Formation of Se atomic layers on Au appears to be a kinetically hindered process, regardless of the electrochemical method used to produce them. This is most evident for the reductive deposition of Se atomic layers from a H_2SeO_3 solution, where the first atomic layer appears to deposit in a UPD peak (in a surface limited reaction) but actually deposits at an overpotential. The study presented here clearly shows multiple Se structures, as previously observe on Au(100). In nearly all cases, domains of more then one structure were present on the surface at a given time, providing further evidence of the importance of kinetics in the electrochemical formation of the Se atomic layers.

All three methods for electrochemically forming Se atomic layers resulted in ordered structures on the Au(111) and Au(110) surfaces. LEED indicated the formation of one ordered Se structure on each plane, a Au(111)(✓3X✓3)R30^0-Se and a Au(110)(2X3)-Se. STM, however, revealed the formation a number of other structures and features, depending on the deposition conditions. At the lowest coverages on Au(111), below 1/4, a large number of small (✓3X✓3)R30^0-Se domains appeared in a "mosaic" structure. Near a coverage of 1/3, the mosaic structure converted to the (✓3X✓3)R30^0 structure. As the (✓3X✓3)R30^0 domains increase in size and coalesce, a number of phase boundaries became evident. To remove the phase

boundaries, whole domains had to shift adsorption sites. This need to shift adsorption site may account for some of the slow deposition kinetics observed.

Under the conditions used to form the (✓3X✓3)R30^0 structure, other features were nearly always present as well. At coverages near 1/3, phase boundary triangles were observed, and at higher coverage domains of Se_8 rings. As the coverage was increased still further, domains of the Se_8 rings dominated, eventually converting to a less well understood structure at still higher coverages, composed of Se clusters. The atomic density of these clusters is unclear.

STM observations on the Au(110) surface confirmed the formation of a Au(110)(2X3)-Se structure at 2/3 coverage, as predicted from LEED and coulometry. In addition, higher coverage structures were observed, including one resembling a honeycomb. One interpretation of the honeycomb structure is that it is composed of chains of Se atoms on the initial (2X3) Se structure. This honeycomb appears to be the start of a second layer of Se, which at still higher coverages, fills in to complete the second layer.

ACKNOWLEDGMENTS

This work was supported in part by the Navy , office of the Chief of Naval Research, under grant # N00014-91-J-1919, and by the National Science Foundation, under grant # DMR-9017431. Their assistance is gratefully acknowledged.

REFERENCES

1. Barren, A.R., *Adv. Mat. For Optics and Electronics* 1995, *5*, 245.

2. Tsuchiya, K.; Sakata, M.;Funyu, A.; Ikoma, H., *Japan. J. Appl. Phys.*, **1995, *34***, 5926.

3. Suggs, D.W.; Stickney, J.L., *J. Phys. Chem.*, **1991,** *95,* 10056.

4. Suggs, D.W.; Stickney, J.L., *Surf. Sci.*, **1993,** *290,* 375.

5. Lister, T.E.; Huang, B.M.; Herrick, R.D., II; Stickney, J.L., *J. Vac. Sci. Tech., B,* **1995,** *13,* 1268.

6. Huang, B.M.; Lister, T.E.; Stickney, J.L., J. Phys. Chem., in preparation.

7. Wei, C.; Myung, N.; Rajeshwar, K., *J. Eloectroanal. Chem.* **1994,** *375,* 109.

8. Feliu, J.M.; Bomez, R.; Llorca, M.S.; Aldaz, A., *Surf. Sci.*, **1993,** *289,* 152.

9. Mattsson, G.; Nyholm, L.; Peter, L.M., *J. Electroanal. Chem.* **1993,** *347,* 326.

10. Kiskinova, M.P.; Szabo, A.; Yates, J.T., *Surf. Sci.*, **1990,** *226,* 237.

11. Kiskinova, M.P.; Szabo, A.; Yates, J.T., *Phys. Rev. Lett.*, **1988,** *61,* 2875.

12. Bravo, B.G.; Michelhaugh, S.L.; Soriaga, M.P.; Villegas, I., Suggs, D.W.; Stickney, J.L., *J. Phys. Chem.*, **1991,** *95,* 5245.

13. McCarley, R.L.; Bard, A.J., *J. Phys. Chem.*, **1991,** *95,* 9618.

14. Gao, X.; Weaver, M.J., *J. Am. Chem. Soc.*, **1992,** *114,* 8544.

15. Gao, X.; Edens, G.J.; Liu, F.C.; Hamelin, A.; Weaver, M.J., *J. Phys. Chem.*, **1994,** *98,* 8086.

16. Gao, X., Edens, G.J.; Weaver, M.J., *J. Phys. Chem.*, **1994,** *98,* 8074.

17. Yamada, T.; Batina, N.; Itaya, K., *Surf. Sci.*, **1995,** *335,* 204.

18. Hwang, R.Q.; Zeglinski, D.M.; Lopez Vazquez-de-Parga, A.; Ogletree, D.F.; Somorjai, G.A.; Salmeron, M.; Denley, D.R., *Phys. Rev. B,* 1991, *44,* 1914.

19. Gao, X.; Zhang, Y.; Weaver, M.J., *J. Phys. Chem.*, **1992,** *96,* 4156.

20. McCarley, R.L.; Kim, Y.T.; Bard, A.J., *J. Phys. Chem.*,**1993,** *97,* 211.

21. Ogletree, D.F.; Ocal, C.; Marchon, B.; Somorjai, G.A.; Salmeron, M.; Beebe, T.; Siekhaus, W., *J. Vac. Sci. Technol. A*, **1990**, *8*, 297.

22. Bedair, S. *Atomic Layer Epitaxy*, Elsevier: New York, 1992.

23. Dapkus, P.D.; Kuech, T.F.; Atomic Layer Growth and Processing, Proc. 222; Materials Research Soc: Pittsburgh, 1991.

24. Kolb, D.M. in *Advances in Electrochemistry and Electrochemical Engineering*, Vol. 11, Eds. H. Gerischer, C.W. Tobias,; Wiley: New York, 1978; p 125.

25. Demir, U.; Shannon, C. *Langmuir*, **1994**, *10*, 2794.

26. Demir, U.; Shannon, C. *Langmuir*, **1996**, *12*, 594.

27. Gregory, B.W.; Stickney, J.L. *J. Electroanal. Chem.*, **1991**, *300*, 543.

28. Villegas, I.; Stickney, J.L. *J. Electrochem. Soc.*, **1992**, *139*, 686.

29. Colletti, L.P.; Tekley, D.; Stickney, J.L. *J. Electoanal. Chem.*, **1995**, *369*, 145.

30. Huang, B.M.; Colletti, L.P.; Bregory, B.W.; Anderson, J.L.; Stickney, J.L. *J. Electrochem. Soc.* **1995**, *142*, 3007.

31. Rhee, C.K.; Huang, B.M.; Wilmer, E.M.; Thomas, S.; Stickney, J.L. *Mater. and Manuf. Process.*, **1995**, *10*, 283.

32. Huang, B.M.; Lister, T.E.; Stickney, J.L. in The handbook of Surface Imaging and Visualization, Ed. Hubbard, A.T., CRC Press: New York, 1995; p. 75.

33. Lister, T.E.; Stickney, J.L. Appl. Surf. Sci., in press.

34. Lister, T.E.; Stickney, J.L. Surf. Sci., in preperation.

35. Soriaga, M.P.; Harrington, D.A.; Stickney, J.L.;Wieckowski, A. *in Modern Aspects of Electrochemistry*, vol. 28, Eds.: Conway, B.E.; Bockris, J.O'M.; White, R.E.; Plenum: New York, 1996, p. 1.

36. Nagahara, L.A.; Thundat, T.; Lindsay, S.M. Rev. *Sci. Instrum.*, **1989, *60,*** 3128

37. Tegart, W.J. McG.; *The Electrolytic and Chemical Polishing of Metals in Research and Industry,* Permangon: Oxford, 1959, p. 62.

38. Greenwood, N.N.; Earnshaw, A. *Chemistry of the Elements,* Permangon: Oxford, 1986, p. 882.

39. Suggs, D.W.; Bard, A.J. *J. Am. Chem. Soc.*, **1994,** *116*, 10725.

FIGURES

Figure 1 Voltammetry of the clean Au tri-crystal in a solution of 1 mM SeO_2 with 20 mM H_2SO_4. Scan rate: 5 mV/sec.

Figure 2 LEED patterns of Se atomic layers on Au(111) and Au(110):
A) Au(111)(✓3X✓3)R30^0 formed by reductive stripping of bulk Se at -0.27 V. Electron energy: 61.4 eV.
B) Au(110)(2X3) formed by reductive stripping of Se UPD at -0.25 V. Electron energy: 64.9 eV.

Figure 3 STM images of structures formed on Au(111) by reductive deposition to the peak of C_1.
A) (✓3X✓3)R30^0 structure.
B) Combination of (✓3X✓3)R30^0 and domains of Se_8 molecules.
C) (✓3X✓3)R30^0 structure with line defects.
D) Se_8 ring domain.
E) Se_8 rings with resolution of individual atoms.

Figure 4 Proposed structures for Se on Au(111).
A) (✓3X✓3)R30^0-Se, 1/3 coverage.
B) Anti-phase boundaries in (✓3X✓3)R30^0 structure.
C) Domain structure of Se_8 molecules.

Figure 5 STM images of Se structures observed at low Se coverage.
A) Image of a low coverage of Se, using harsh tunneling conditions.
B and C) Images of Se mosaic structure, observed using a high tunneling resistance.

Figure 6 STM images of Se structures formed above 1/2 coverage.
A) Se structure formed by reductive deposition to between C_1 and C_2 (Figure 1).
B) Zoom of A).
C) STM image of Se chain structure, formed near a coverage of 1 monolayer.
D) Image of Se pit and chain structure, near a coverage of 1.25 monolayers.

Figure 7 Sequence of images for a Se covered electrode in 20 mM H_2SO_4, taken at the following potentials:
A) -0.20 V, the initial potential.
B) -0.40 V.
C) -0.50 V.
D) -0.50 V, zoom of image in (C).
E) -0.70 V

Figure 8 Images of Se deposited on Au(110).
A) (3X2) structure formed by reductive deposition to the peak of C_1.
B) (3X2) structure formed by oxidative stripping at -0.55 V.
C) Se structure observed on Au(110) surface at a coverage above 1 monolayer.

Figure 9 Proposed structure for Au(110)(2X3), at 2/3 coverage.

Lister et. al Figure #1

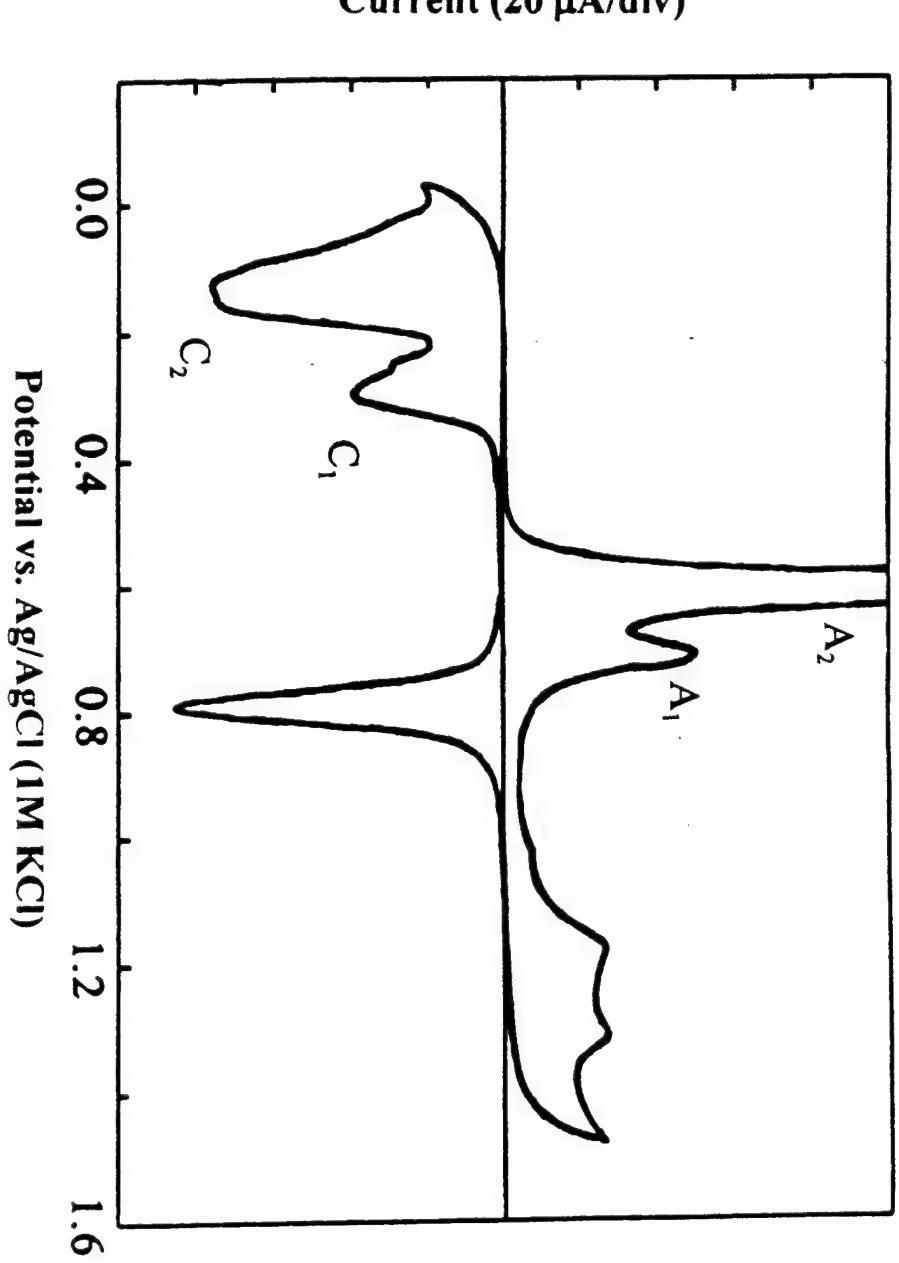

Lister et al #2A

Lister et. al
Figure 2B

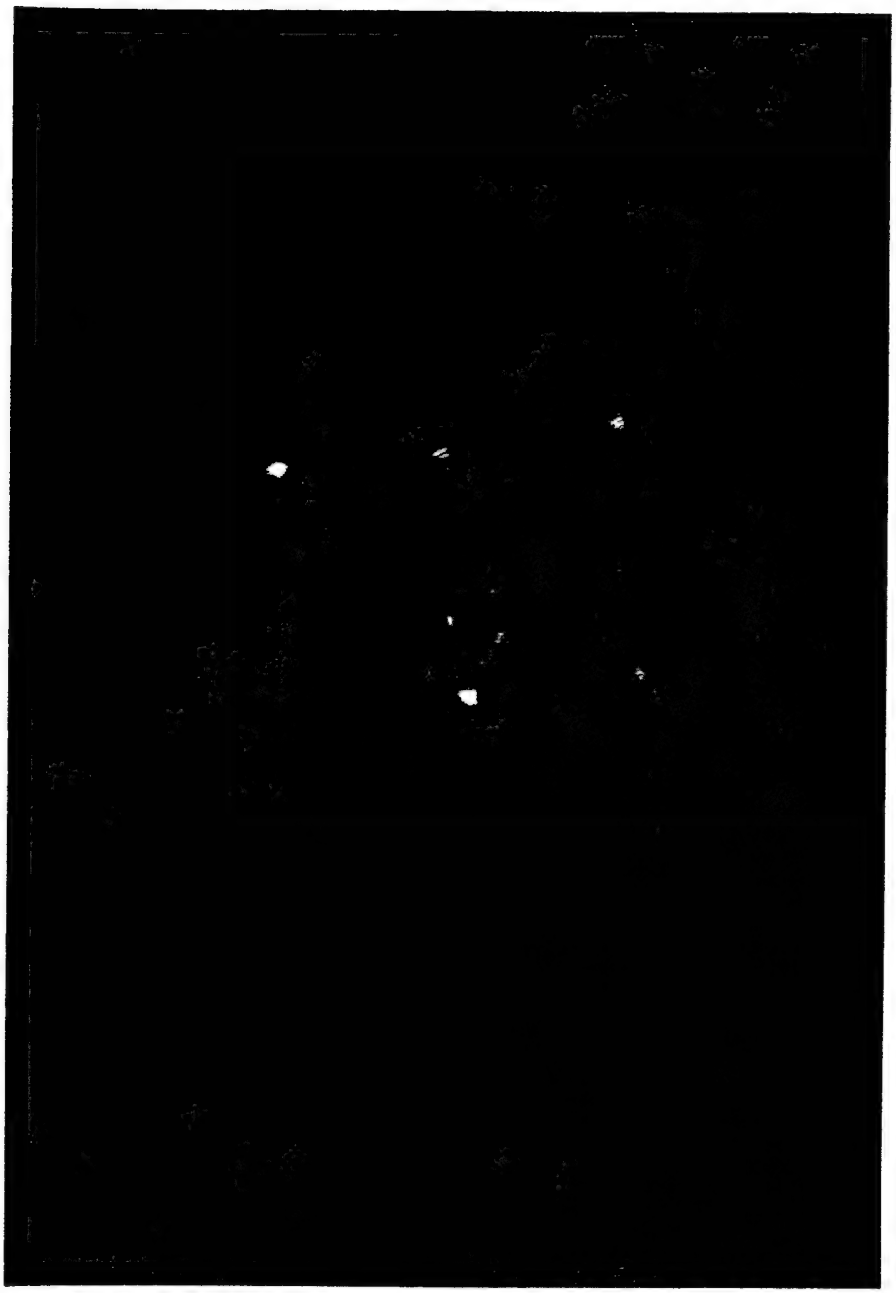

Figure 3A, B
-ister et al.

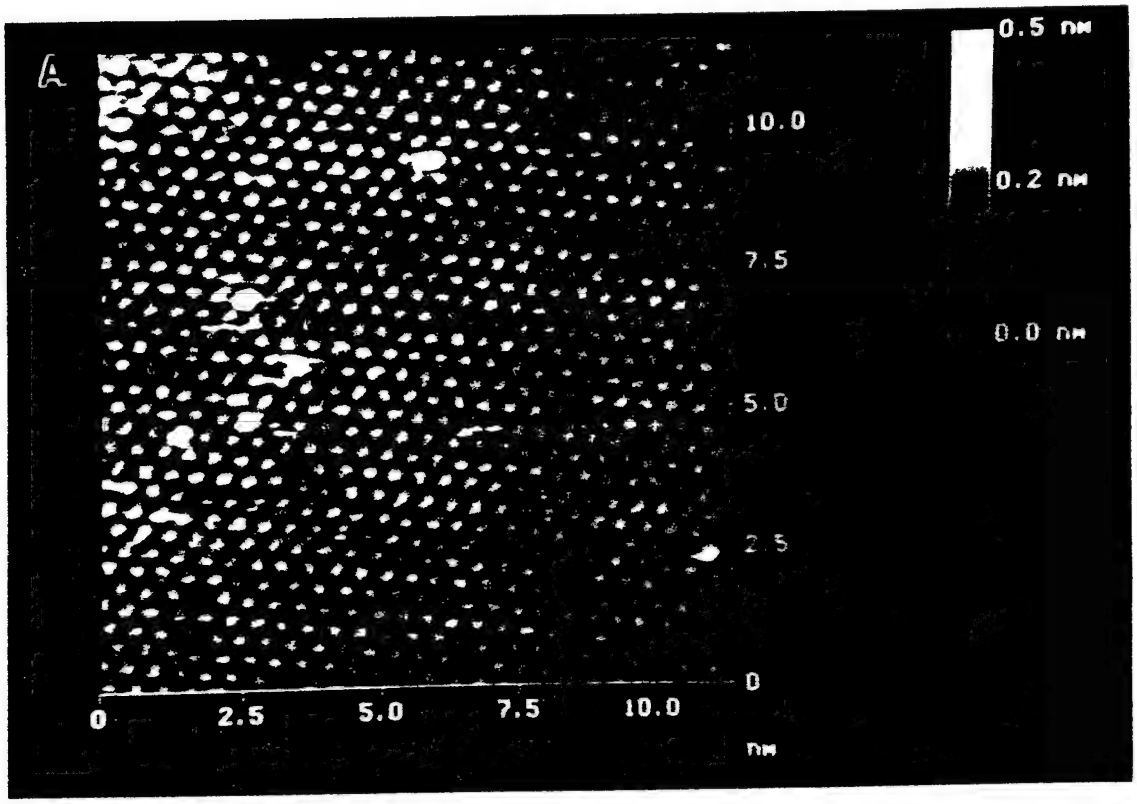

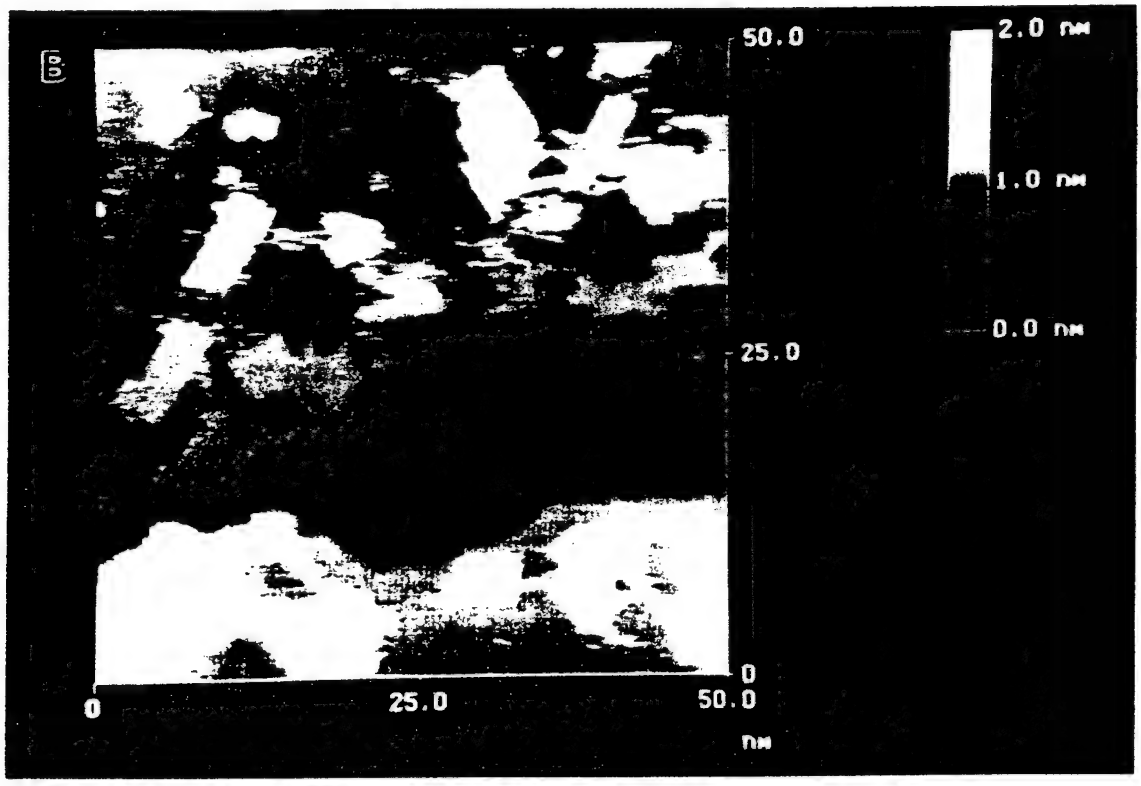

isker et. al.
igure 3C and D

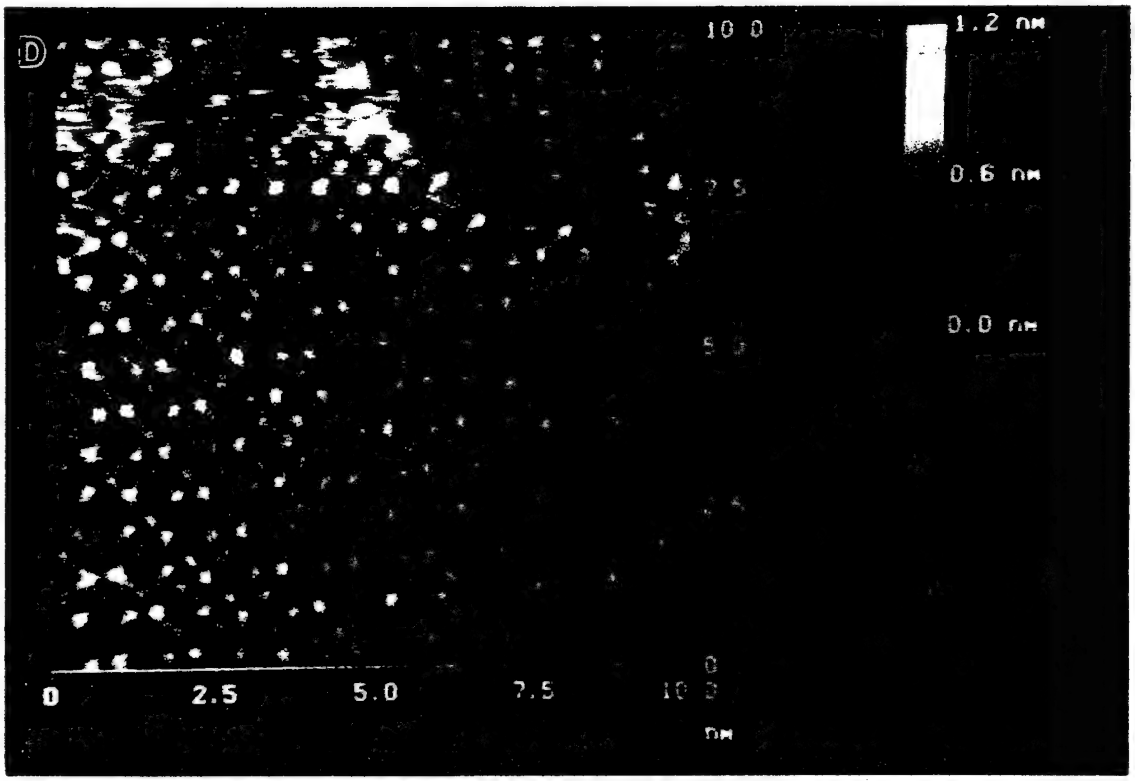

.ister of ah
igure 3E

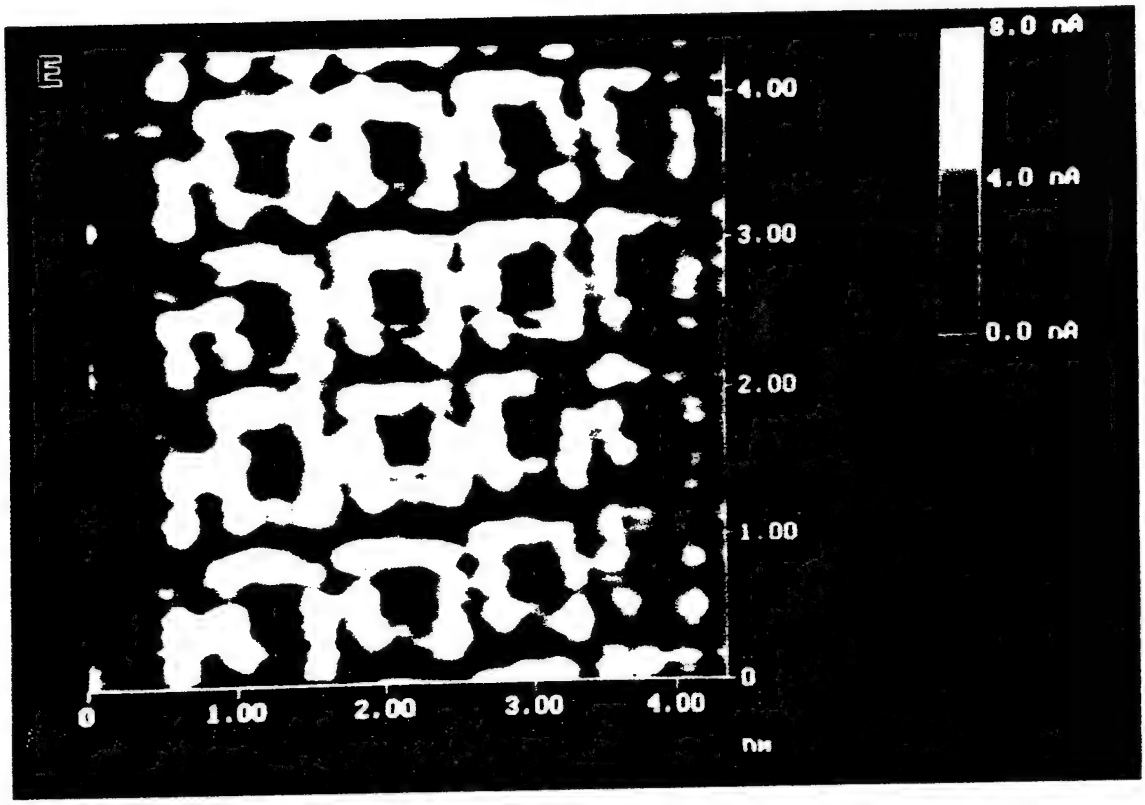

Figure 4A
Sister et al.

A.

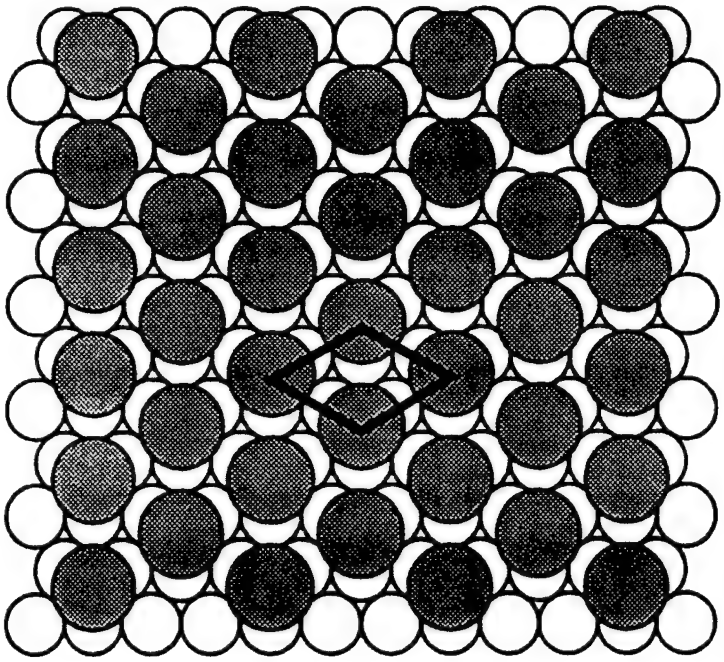

igure 4B
ister et. al.

B.

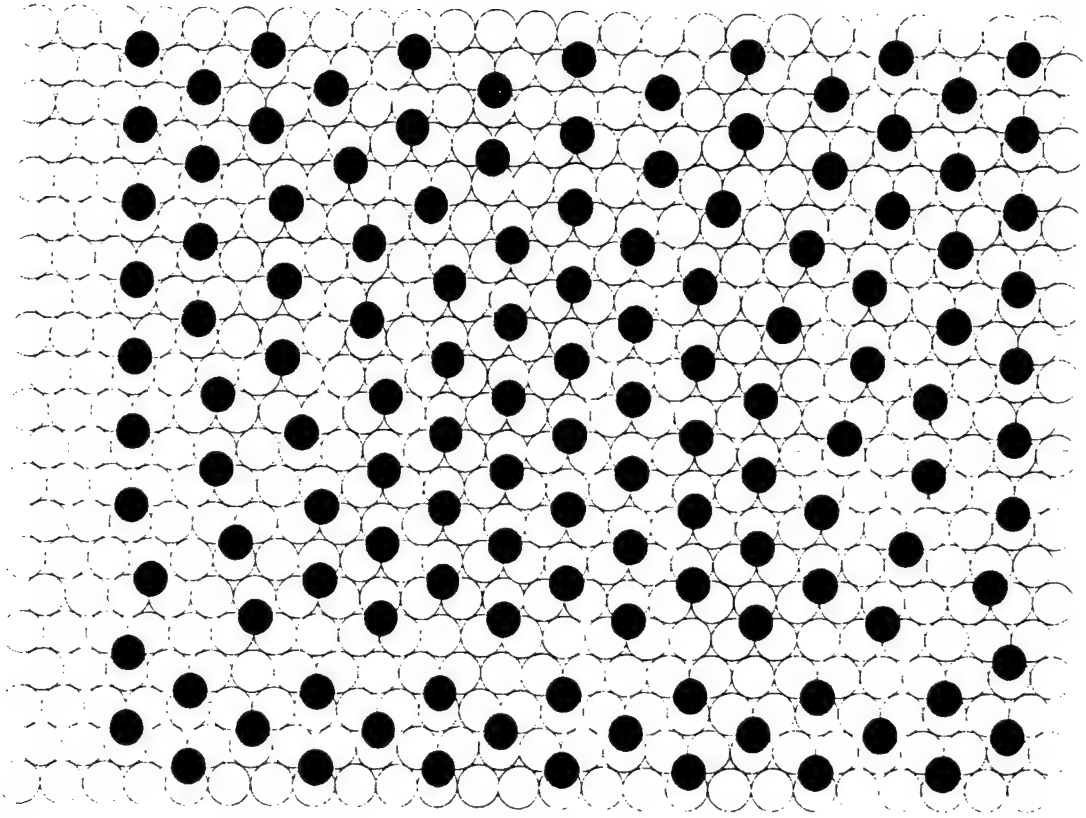

Figure 4C
Listi et al.

C.

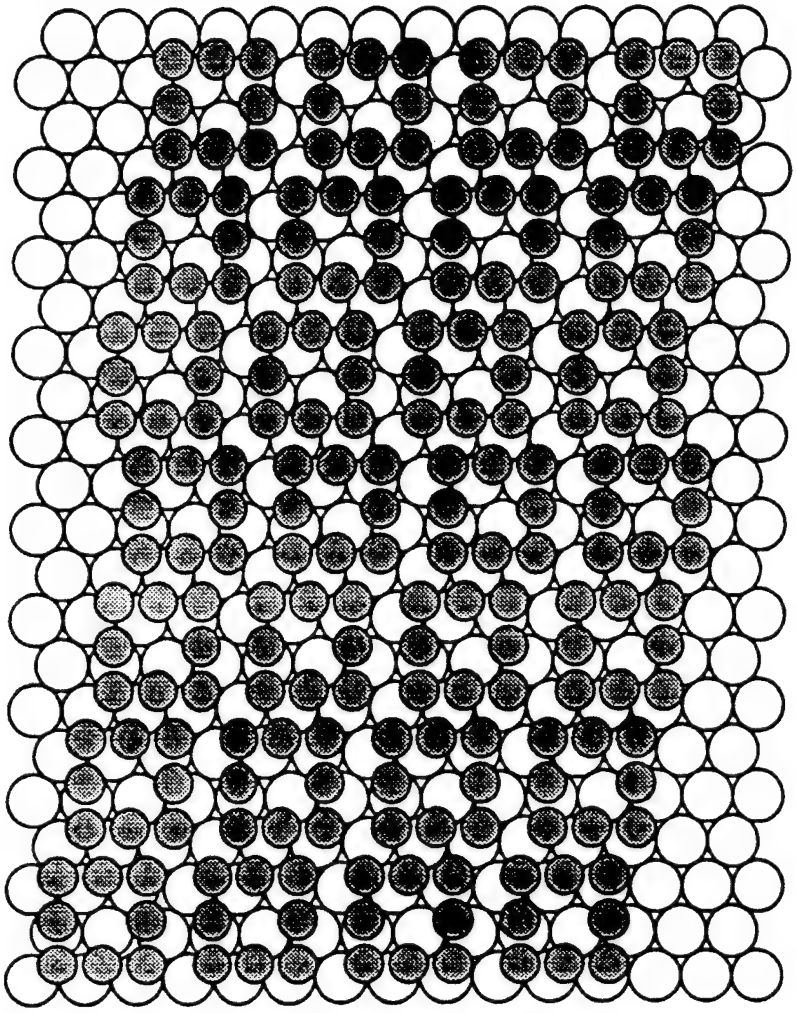

Figure 5 A and B
Foster et al.

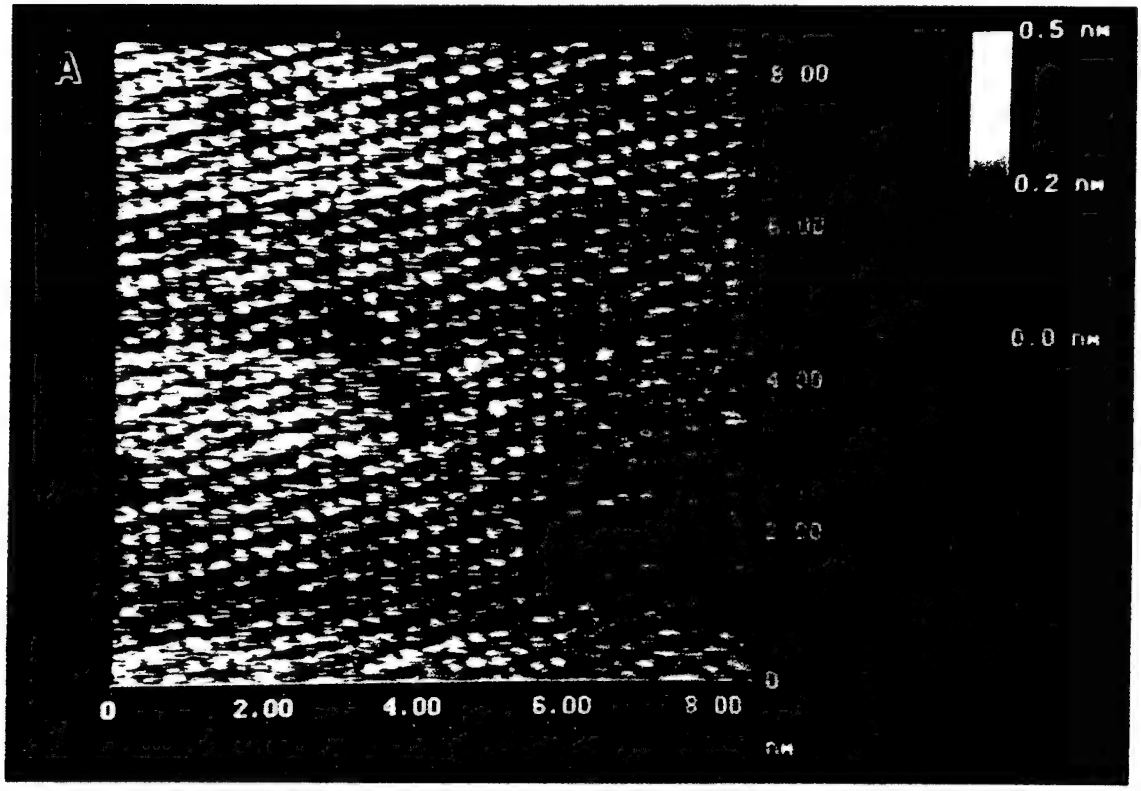

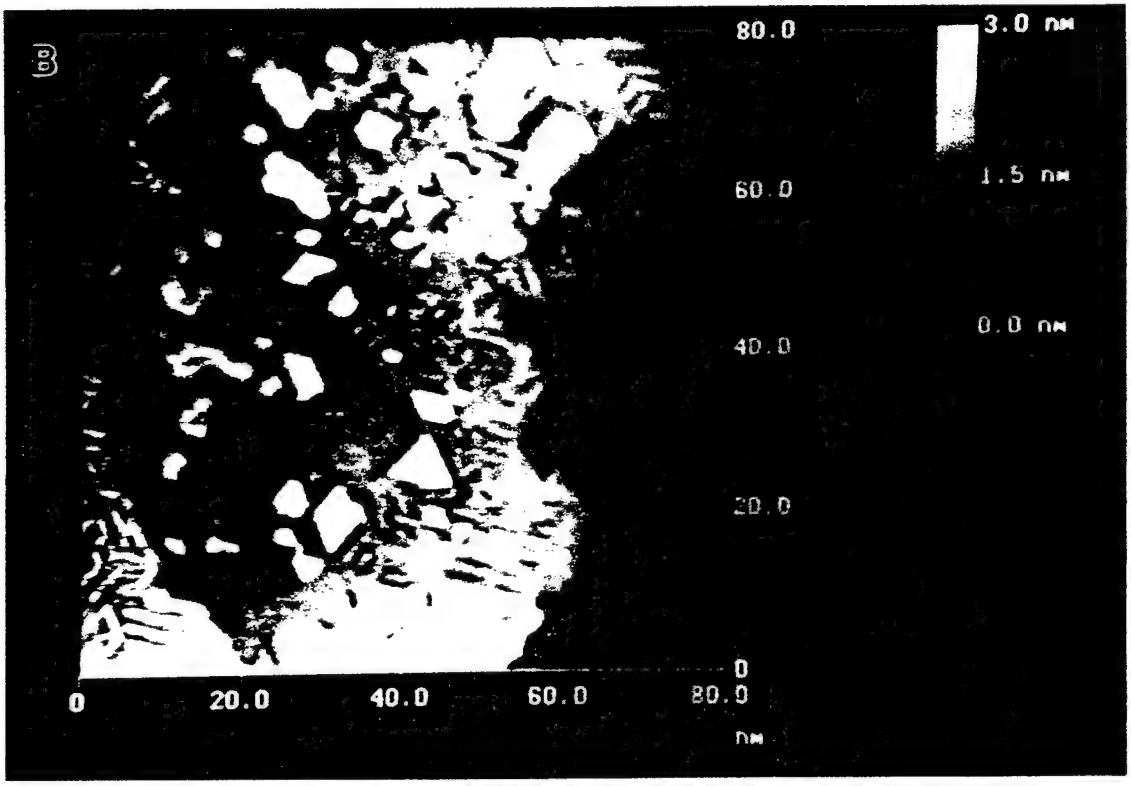

Figure 5C
-Isler et. al.

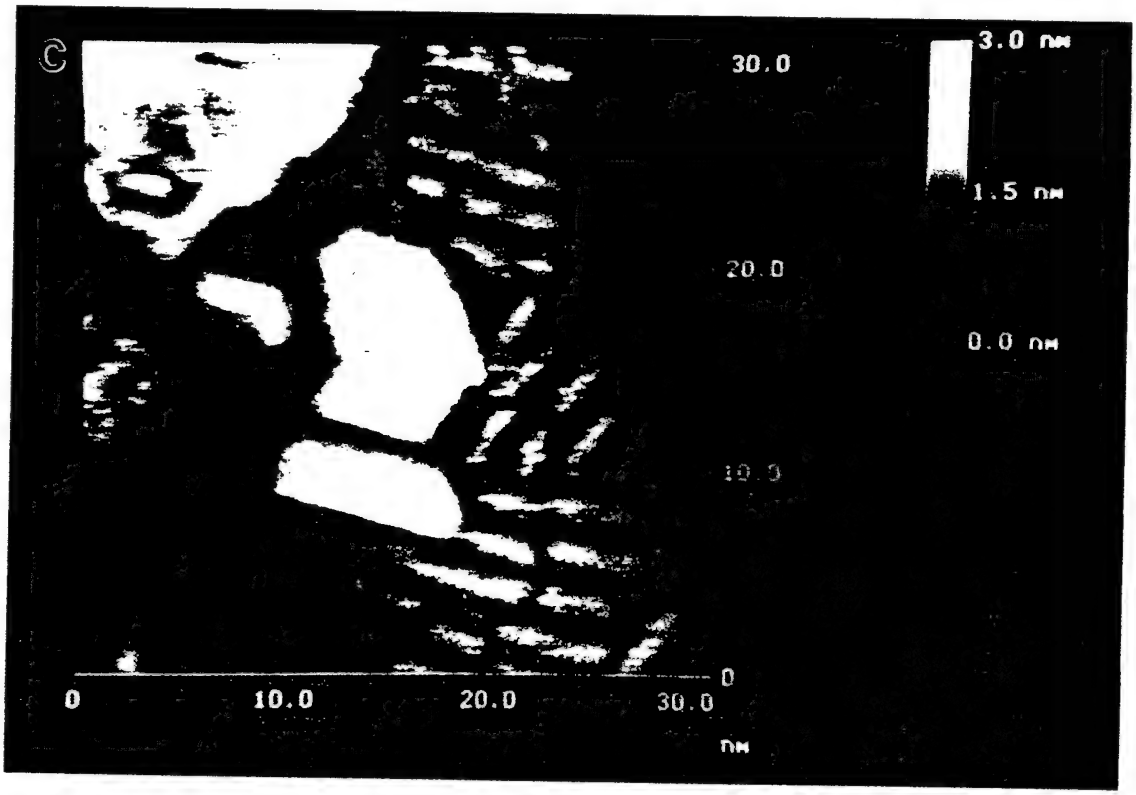

Figure 6 A and B
Lisko et al.

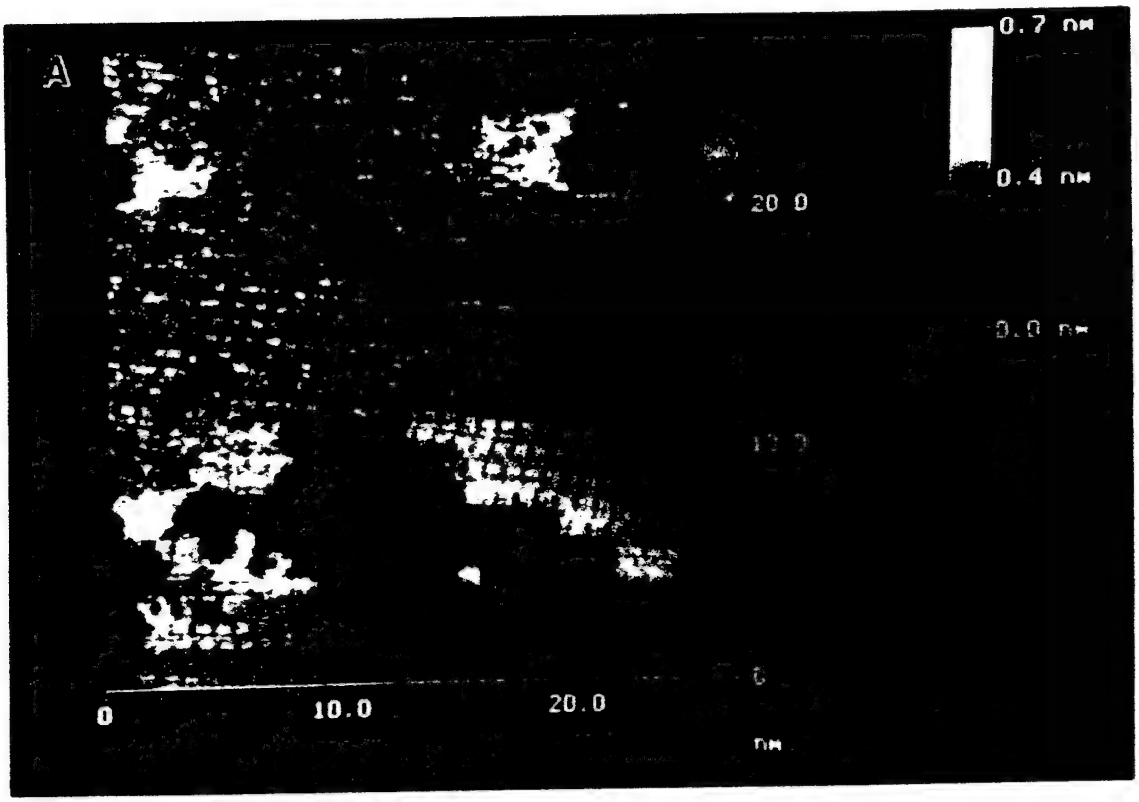

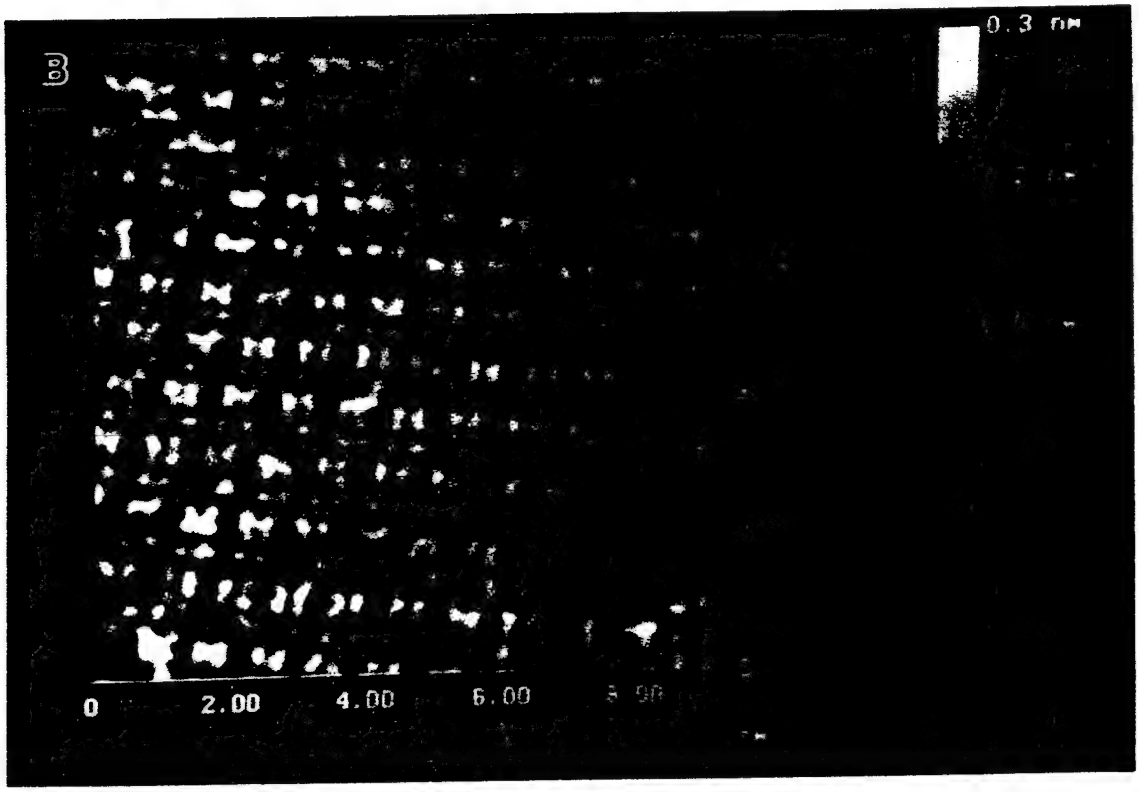

Figures 6C and 6D
Ishii et al.

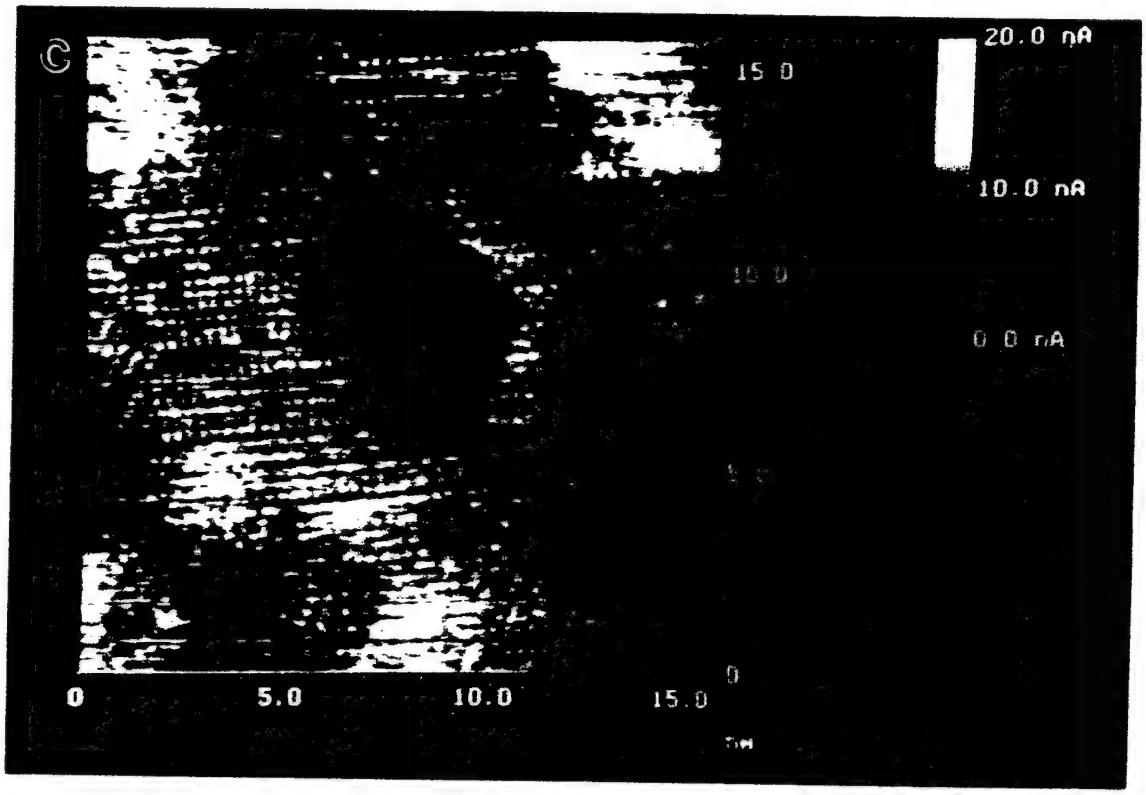

Figure 7A and 7B
-ister et al

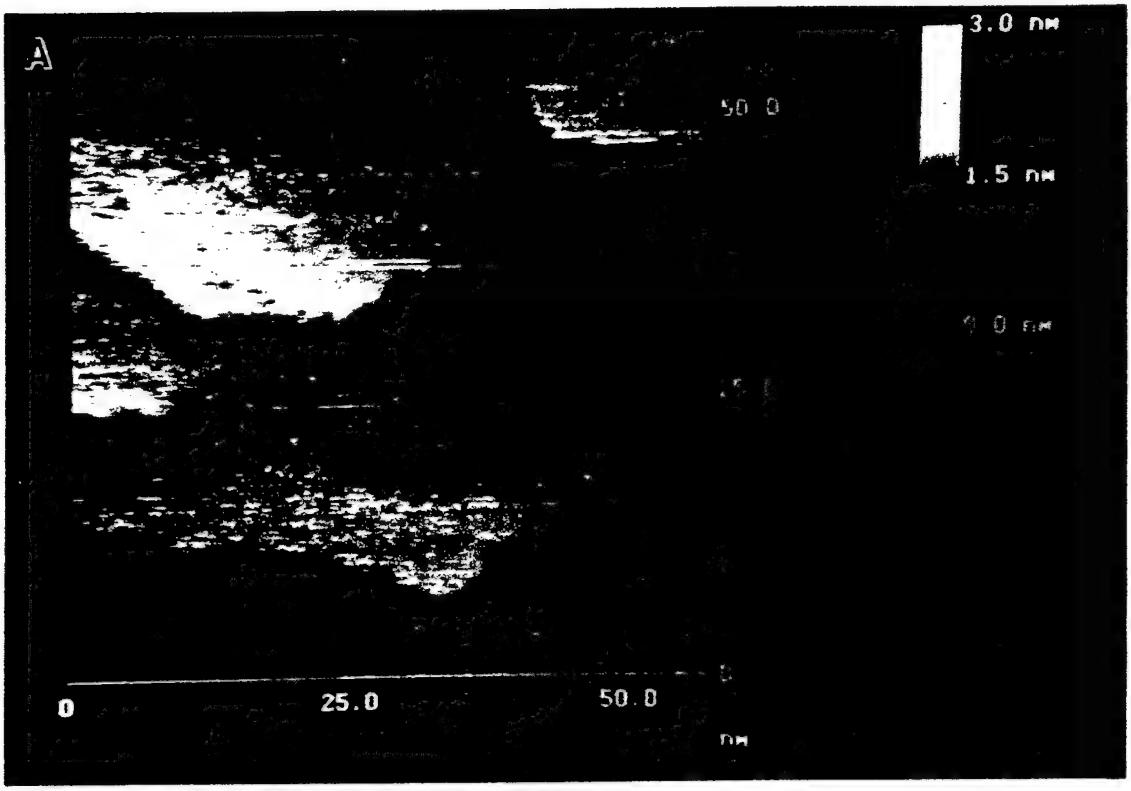

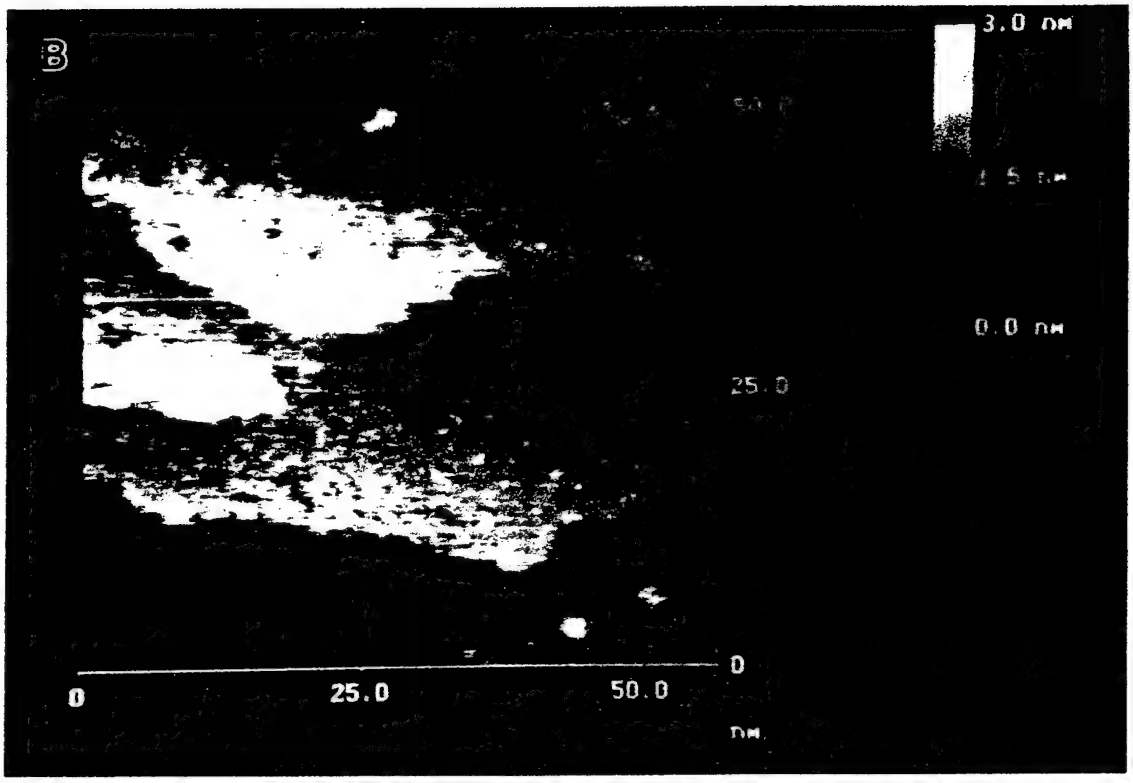

Figure 7C and 7D
"Lister et. al.

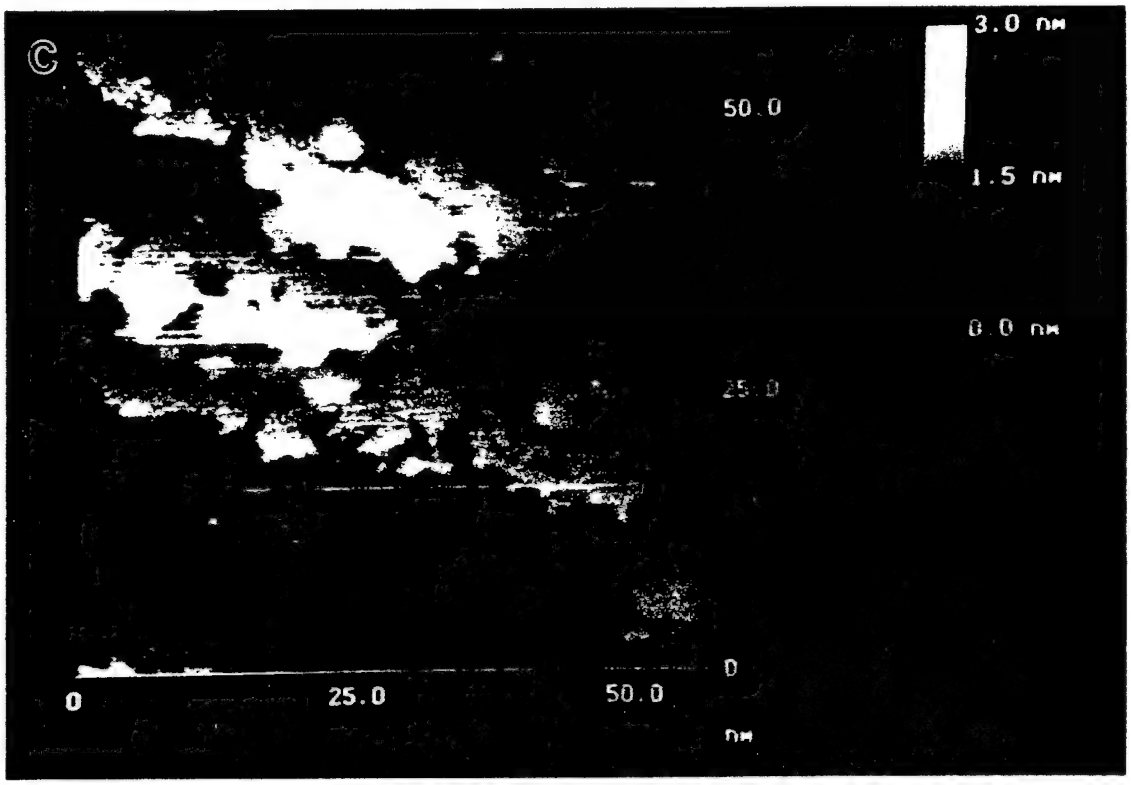

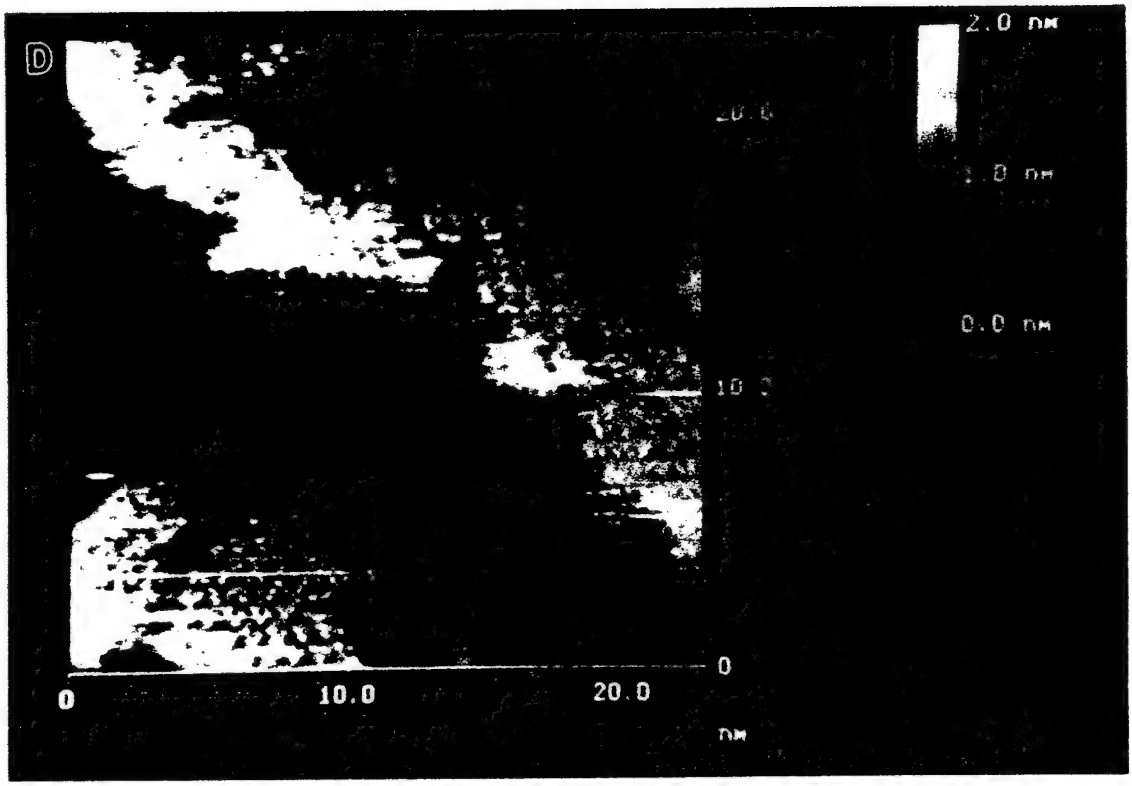

Figure 7E
Lister et al.

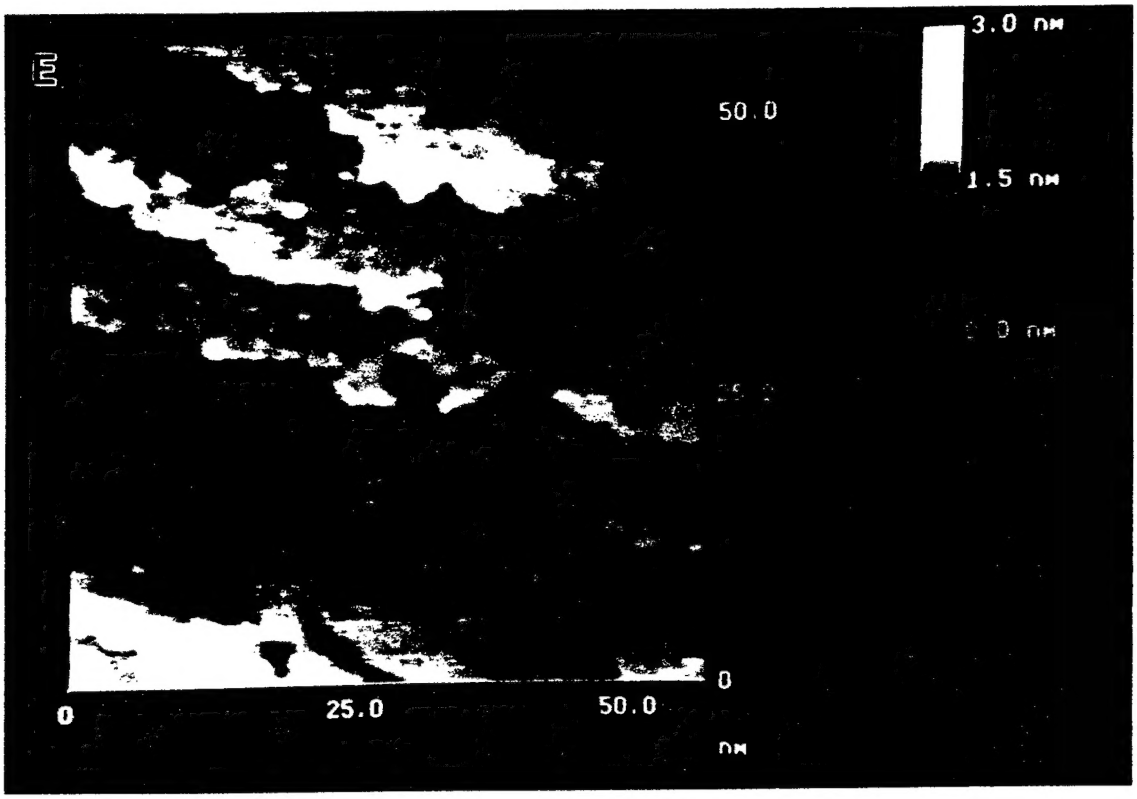

Figure 8A and 8B
Baker et. al.

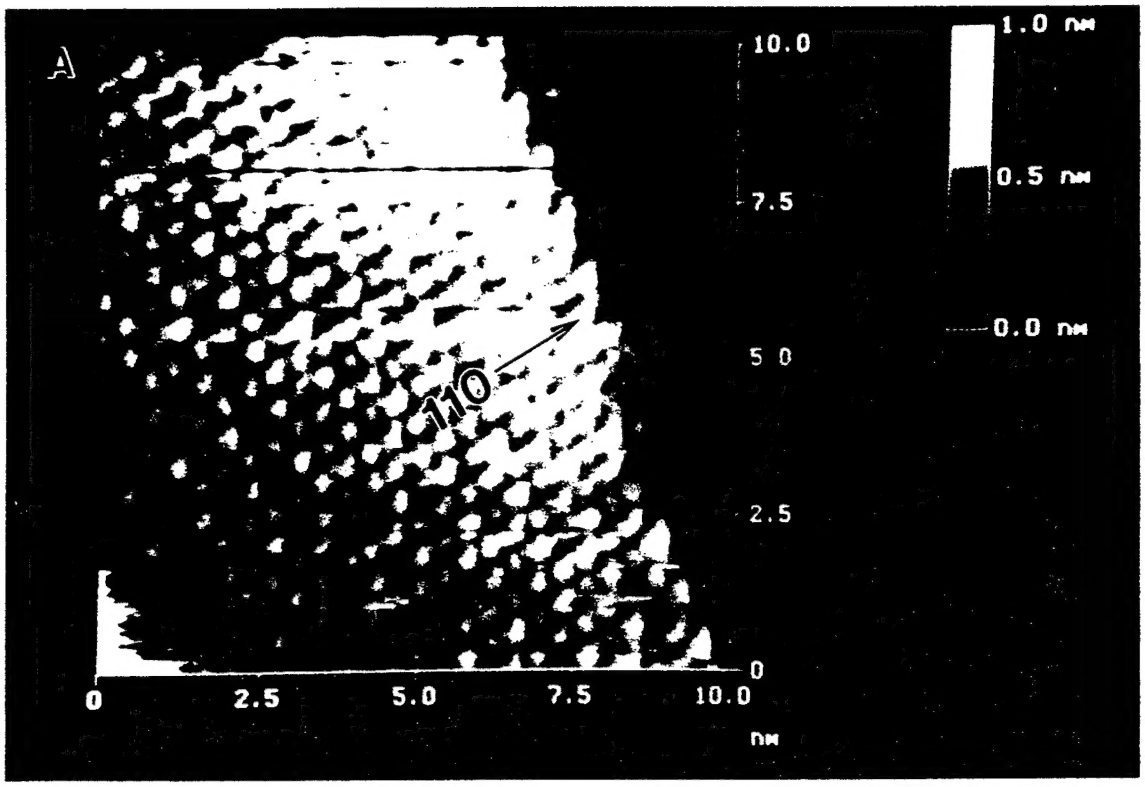

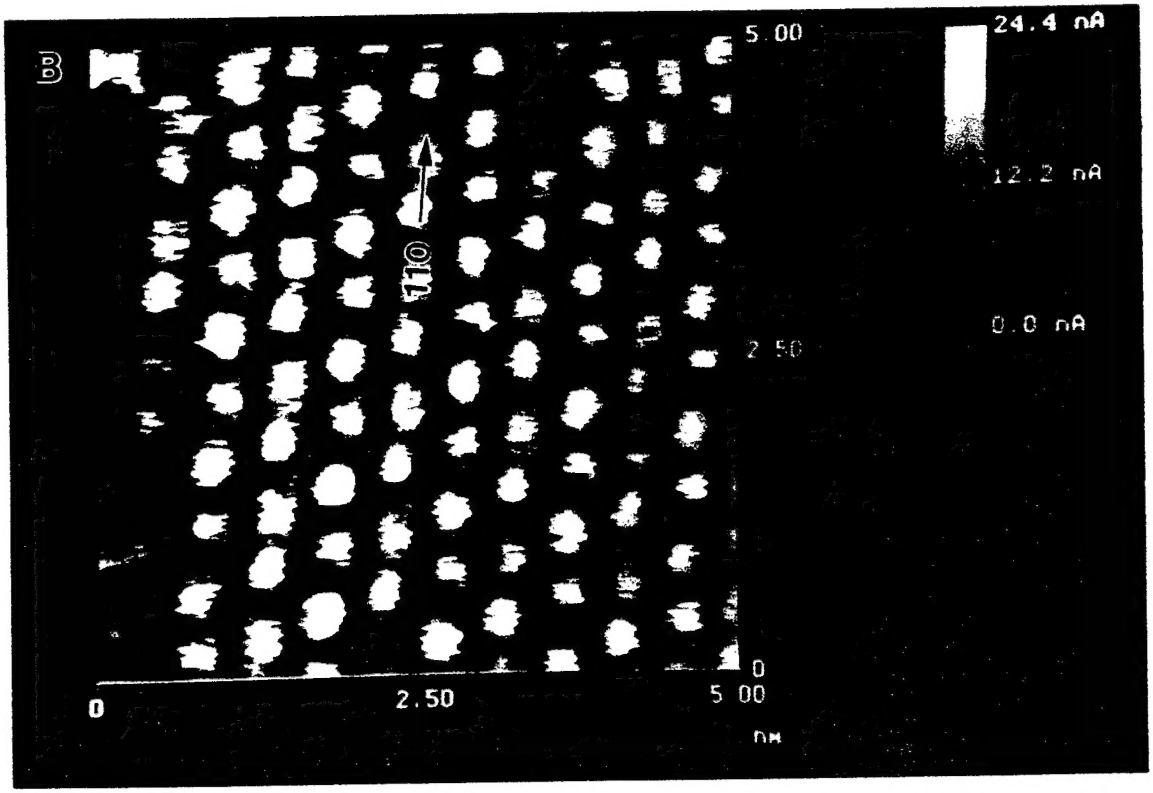

Figure 8C
-ister et. al.

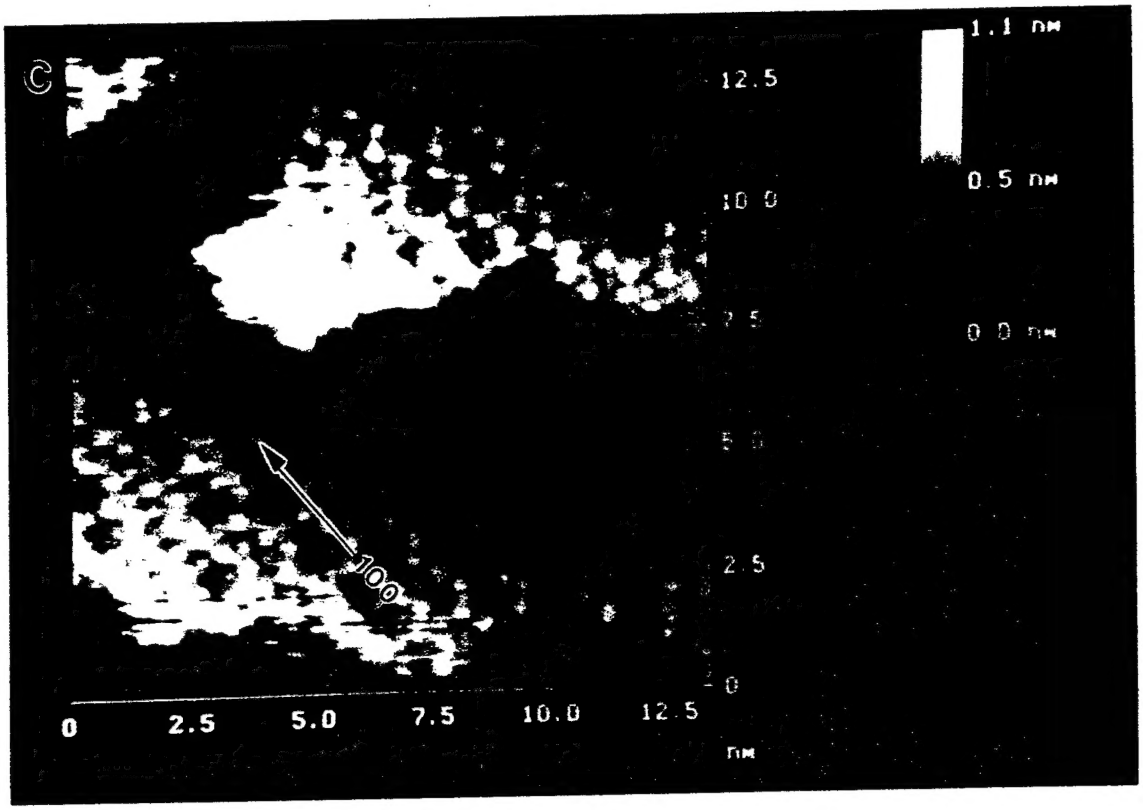

Figure 9
Wister et. al.